

13th CIRP Conference on Intelligent Computation in Manufacturing Engineering, CIRP ICME '19

# Aluminium foam production control by using a combined fuzzy-genetic algorithm model

Gennaro Salvatore Ponticelli<sup>a,b,\*</sup>, Stefano Guarino<sup>b</sup>, Oliviero Giannini<sup>b</sup>, Flaviana Tagliaferri<sup>b</sup>,  
Simone Venettacci<sup>b</sup>, Federica Trovalusci<sup>a</sup>

<sup>a</sup>University of Rome 'Tor Vergata', Department of Enterprise Engineering, Via del Politecnico, 1, 00133, Rome, Italy

<sup>b</sup>University of Rome 'Niccolò Cusano', Department of Engineering, Via Don Carlo Gnocchi, 3, 00166, Rome, Italy

\* Corresponding author. Tel.: +39-0672597168. E-mail address: [gennaro.ponticelli@unicusano.it](mailto:gennaro.ponticelli@unicusano.it)

## Abstract

This study deals with the proposal of a combined fuzzy-genetic algorithm model able to describe the inherent uncertainties related to the manufacture of aluminium foams by using the dissolution and sintering process. The combined method allows taking into account both the uncertainty related to the model and the statistical process variability, with the aim of controlling the capability of this material at absorbing compression energy, for different set of process parameters. The use of genetic algorithms allows the optimization of the fuzzy supports in order to take into account most of the experimental data in combination with the smallest uncertainty.

© 2020 The Authors. Published by Elsevier B.V.

This is an open access article under the CC BY-NC-ND license (<http://creativecommons.org/licenses/by-nc-nd/4.0/>)

Peer review under the responsibility of the scientific committee of the 13th CIRP Conference on Intelligent Computation in Manufacturing Engineering, 17-19 July 2019, Gulf of Naples, Italy.

*Keywords:* Fuzzy logic; Genetic algorithm; Transformation method; Metal foams; DSP

## 1. Introduction

Optimization in engineering problems has always been of great interest for solving complex and nonlinear real-world problems [1–3]. Among the available computational methods that can be used to solve optimization problems in many fields such as engineering and computer science [4–9], economic management and supply chain management [10], empirical methods are considered particularly useful tools, and very often the only available methods that can be used to speed up the characterization of the processes and therefore their optimization. This is due to the strong dynamic nature of the processes which are characterized by a high number of parameters and possible interactions among them. It is worth to state here that these empirical models exist only thanks to the experiments and are valid only within the space that is tested. In fact, they are exclusively built and then validated on the basis of the experimental findings, within the intervals of the investigated parameters.

In general, the decisions to be made to set-up the process are complex, since a wide range of alternative options must be evaluated, and the choice of the best one is frequently made on a set of conflicting criteria [11–13]. There are very different decision-making situations in the manufacturing environment and the evaluation of alternative process designs in order to meet the productivity and final quality requirements is one of the most relevant. In order to obtain effective operative and applicable solutions, we must consider that there will be aspects we are not aware of, i.e. that we do not know for whatever reason, among which are the lack of knowledge or the ignorance of what we do not know [14]. For this reason, there is the need for mathematical tools able to guide the decision-making process in environments characterized by high and different sources of uncertainty. The inherent attitude of fuzzy logic to perform decision-making and deduce control actions under complex and uncertain environments [15] has led to the study of a new field of decision analysis, the fuzzy decision-making. In particular, the fuzzy technique is able to take into account both the random error, e.g. that is associated

to the variability of the process, and the systematic error, e.g. that is due to the simplification introduced in the model thus involving in lack of knowledge. The fuzzy model is therefore able to propagate all the sources of uncertainty at the input level to the output quantities.

In the last decades, metal foams have become increasingly attractive for their interesting physical, mechanical, thermal, electrical and acoustic properties [16–20]. Foam combines part of the characteristics of a bulk metal with the structural advantages of a foam, offering potential for lightweight structures, for energy absorption, and for thermal management. Both the attention and the progress in crashworthiness of vehicles have experienced a significant improvement, focusing the design on the passenger safety. The current philosophy adopted in the automobile industry is to structurally harden the passenger compartment against collapse and intrusion. Then, the features of metallic foams make them suitable to applications requiring high stiffness-to-weight ratio and efficient energy absorption. The challenge is to employ these innovative materials in a controlled manner [21]. The improvement of many manufacturing techniques has allowed the development of different foaming processes, making it possible to easily control the shape and distribution of the space-holders as well as the morphology of the porosity in the foams, promoting an improved repeatability, which allows designing the material properties by simply choosing the characteristics and the amount of the space-holder [22].

Among the different process-routes developed so far, the Dissolution and Sintering Process (DSP) is a valuable alternative thanks to its flexibility and capability to guarantee an easy control of the shape and distribution of the space-holders as well as the morphology of the porosity in the foams [22]. However, the need to tune one by one all the process parameters in order to meet the desired requirements for the considered application, consumes a lot of resources in terms of time, efforts and money. For this reason, empirical methods can be applied in order to find the optimal operational parameters. On the other hand, since this kind of process suffers from a strong process variability in terms of density of pores and their distribution, traditional statistical approaches may fail at identifying which factors are the most influential. On the other hand, models that include all the factors and their interactions may be unsuitable for modelling and prediction, due to their complexity. Moreover, even complicated models still will represent only the median process leaving the user with little information about the dispersion around the mean. For this reason, more uncertain models based on expert systems such the fuzzy logic can be considered a valuable alternative for modelling the experimental data and for simulation purposes.

In this context, the present study is aimed at proposing a fuzzy uncertain model able to describe the inherent uncertainties related to a DSP foam manufacturing process, with the aim of predicting the resulting absorbing energy properties and the compressive deformation behaviour, for different set of process parameters. In particular, the use of the genetic algorithm allows the optimization of the support of the fuzzy model in order to take into account most of the experimental data in combination with the smallest

uncertainty level. Then, the input uncertainty, related to both the process variability and the chosen model, is propagated to the output variables by the Transformation Method [23]. Finally, the process maps obtained by the application of the fuzzy model is used to select operational parameters in order to satisfy the requirement of the highest energy absorption and the lowest deformation in combination with the lowest level of uncertainty.

## 2. Methods

The Dissolution and Sintering Process [22] consists of four main steps (see Fig. 1): i) mixing the starting metal powder with the Space-Holder Particles (SHP); ii) compacting the mixture in order to obtain a green compact; iii) dissolution of the SHP with an appropriate solvent in order to obtain a cellular structure; iv) sintering of the latter structure to produce metallurgical bond among the metallic powders.

The overall mechanical properties of the samples were characterized by means of compression tests performed with a static test machine (MTS model Alliance RT/50). Load speed was set at 1 mm/min. Fig. 2 reports the typical output of the compression tests performed.

As shown in Fig. 2, the compressive deformation behaviour  $\Delta L$  is the sum of the deformation during the elastoplastic and extended plateau zone, while the mechanical energy absorption  $E$  is represented by the dashed area.

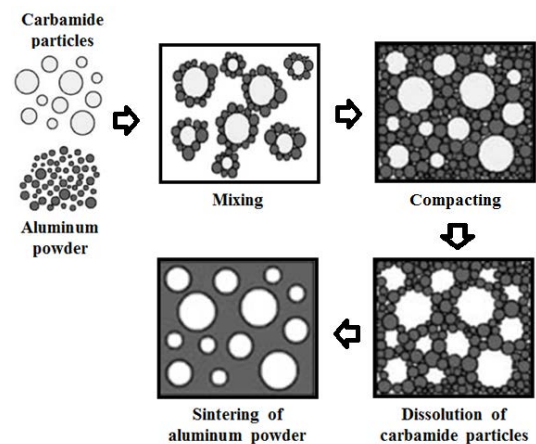


Fig. 1. Highlights of the DSP process.

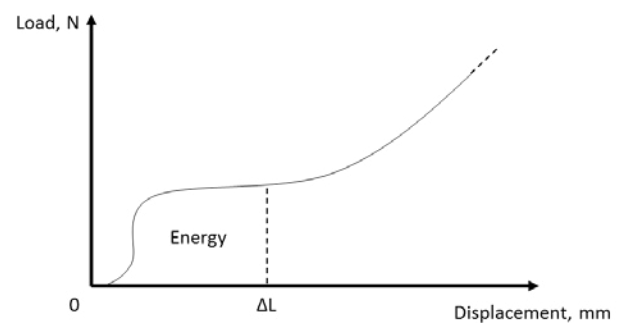


Fig. 2. Typical output of the compression tests performed.

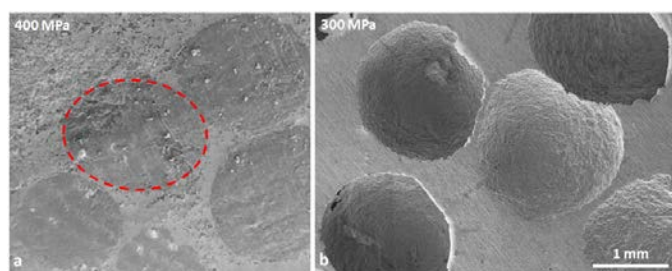


Fig. 3. SEM images of an open cell aluminium foam: a) compacted aluminium powders with carbamide particles; b) precursor after the dissolution process. The dashed red circle highlights the ovalization of the carbamide particles occurring for increasing compaction pressure.

Among the large number of process parameters, the weight percentage of carbamide particles ( $C_{\%}$ ), their mesh size ( $C_{MS}$ ) and the compaction speed ( $S$ ) were varied according to the developed full factorial plan based on Design of Experiment, which is reported in Table 1. Moreover, in order to assess the process variability, 5 repetitions were performed for each experimental scenario investigated. It is worth to note that in this study, among the pressures examined in [22], only the value of 300 MPa was maintained, because of the change in shape of the carbamide particles when compacted under higher pressure values (i.e. 400 and 500 MPa), which does not ensure the realization of homogenous spherical-like cells in the foams (as highlighted in Fig. 3 by the dashed red circle).

Table 1. Full factorial plan: 3 terms of  $C_{\%}$  · 3 terms of  $C_{MS}$  · 2 terms of  $S$  · 5 replications = 90 tests.

Control factor	Value			Unit
$C_{\%}$	40	50	60	wt%
$C_{MS}$	12 (0.84)	16 (1.19)	20 (1.68)	-( $\mu$ m)
$S$	1		10	mm/min

### 3. Results and Discussion

#### 3.1. Experimental and Statistical Analysis

The analysis of the experimental results was carried out by means of the ANOVA test, shown in Table 2 and Table 3, in which the significant effects (i.e.  $p$ -value < 0.05,  $\Pi$  > 5%,  $F$ -value > 3.984 for 1-DoF,  $F$ -value > 3.134 for 2-DoF and  $F$ -value > 2.594 for 4-DoF) are highlighted by the bold text.

Table 2. ANOVA table for the absorbed energy.

Source	DoF	Adj.SS	Adj.MS	F-value	p-value	$\Pi$ (%)
$C_{\%}$	2	2.82073	1.41036	<b>4045.90</b>	<b>&lt; 0.001</b>	<b>50.02</b>
$C_{MS}$	2	0.45969	0.22985	<b>659.35</b>	<b>&lt; 0.001</b>	<b>8.15</b>
$S$	1	0.42745	0.42745	<b>1226.22</b>	<b>&lt; 0.001</b>	<b>7.58</b>
$C_{\%} * C_{MS}$	4	0.35117	0.08779	<b>251.85</b>	<b>&lt; 0.001</b>	<b>6.22</b>
$C_{\%} * S$	2	0.44267	0.22134	<b>634.94</b>	<b>&lt; 0.001</b>	<b>7.85</b>
$C_{MS} * S$	2	0.92855	0.46427	<b>1331.86</b>	<b>&lt; 0.001</b>	<b>16.47</b>
$C_{\%} * C_{MS} * S$	4	0.18399	0.04600	131.95	< 0.001	3.26
Error	72	0.02510	0.00035	-	-	0.45
Total	89	5.63934	-	-	-	-

Table 3. ANOVA table for the compressive deformation.

Source	DoF	Adj.SS	Adj.MS	F-value	p-value	$\Pi$ (%)
$C_{\%}$	2	0.75359	0.37679	<b>919.91</b>	<b>&lt; 0.001</b>	<b>14.36</b>
$C_{MS}$	2	0.64436	0.32218	<b>786.58</b>	<b>&lt; 0.001</b>	<b>12.28</b>
$S$	1	0.11053	0.11053	269.86	< 0.001	2.11
$C_{\%} * C_{MS}$	4	2.03194	0.50799	<b>1240.20</b>	<b>&lt; 0.001</b>	<b>38.72</b>
$C_{\%} * S$	2	0.39850	0.19925	<b>486.45</b>	<b>&lt; 0.001</b>	<b>7.59</b>
$C_{MS} * S$	2	0.16417	0.08209	200.41	< 0.001	3.13
$C_{\%} * C_{MS} * S$	4	1.11515	0.27879	<b>680.64</b>	<b>&lt; 0.001</b>	<b>21.25</b>
Error	72	0.02949	0.00041	-	-	0.56
Total	89	5.24774	-	-	-	-

As reported in the latter tables, the weight percentage of carbamide particles was found to be of major influence for both the energy and the compressive deformation. In particular, increasing  $C_{\%}$  means decreasing the amount of energy the foam can absorb during its compression. This result can be attributed to the loss of rigidity of the structure due to the massive presence of porosities [24]. On the other hand, the low value of contribution percentage of mesh size of carbamide particles could suggest the rather low capability of such experimental factor to induce systematic variation in the energy absorption and deformation. Even compaction speed was found to be characterized by a very low contribution, especially for the compressive deformation. In any case, the understanding of which factor and/or interaction is significant or not cannot be drawn by a simple examination of  $p$ -values,  $F$ -values and related contribution percentages. In fact, experimental data are nearly homoscedastic. This determines Fischer's factors largely bigger than the corresponding values tabulated and do not allow to deduce conclusions about the meaningfulness of each investigated factor and interaction [25]. For this reason, in the present study, a sophisticated model based on fuzzy logic with further support of genetic algorithms, with the aim of minimizing the conservativeness of the model itself, has been selected for modelling the experimental data and for simulation purposes.

#### 3.2. Fuzzy Uncertain Modelling

Based on the results of the ANOVA test, an empirical model of the foams manufacturing process has been proposed. Basically, the numerical formulation can be drawn as follows:

$$\begin{aligned}
 Out = & k_0 + k_1 \cdot C_{\%} + k_2 \cdot C_{MS} + k_3 \cdot S + \\
 & + k_4 \cdot C_{\%} \cdot C_{MS} + k_5 \cdot C_{\%} \cdot S + k_6 \cdot C_{MS} \cdot S + \\
 & + k_7 \cdot C_{\%} \cdot C_{MS} \cdot S
 \end{aligned} \quad (1)$$

In the latter equation,  $Out$  represents the output variable, while the empirical coefficients  $k_0$ ,  $k_1$ ,  $k_2$ ,  $k_3$ ,  $k_4$ ,  $k_5$ ,  $k_6$ , and  $k_7$  are the calibration coefficients of the model, which were determined by nonlinear multiple regression analysis based on the whole experimental data set (see Table 4).

Table 4. Calibration coefficients.

Calibration coefficient	Value	
	Absorbed energy	Deformation
$k_0$	-1.505162	-2.230613
$k_1$	0.022814	0.0476638
$k_2$	0.157267	0.1306982
$k_3$	0.347218	0.4866902
$k_4$	-0.002149	-0.0022299
$k_5$	-0.004427	-0.0098813
$k_6$	-0.015723	-0.0280976
$k_7$	0.000176	0.0005809

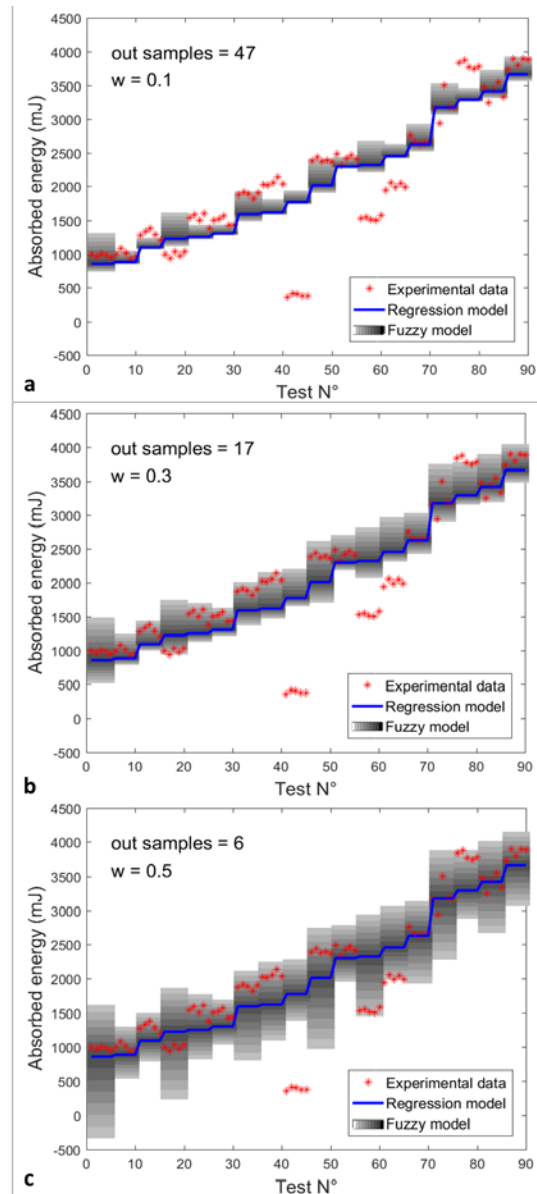
Then, the regression model described by the Equation 1 was considered as the starting model for the development of the related fuzzy regression model, which is written as follows:

$$\begin{aligned} Out^* &= k_0^* + k_1^* \cdot C_{\%} + k_2^* \cdot C_{MS} + k_3^* \cdot S + \\ &+ k_4^* \cdot C_{\%} \cdot C_{MS} + k_5^* \cdot C_{\%} \cdot S + k_6^* \cdot C_{MS} \cdot S + \\ &+ k_7^* \cdot C_{\%} \cdot C_{MS} \cdot S \end{aligned} \quad (2)$$

In Equation 2, all the coefficients are expressed as triangular fuzzy numbers and they are described by 8  $\alpha$ -cuts and the interval at each  $\alpha$ -level is discretized with 2 points. For each  $\alpha$ -cut, the transformation method requires, in a combinatorial scheme, the evaluation of the number of points within the  $\alpha$ -cut to the power of the number of fuzzy parameters, 8 in this case, leading to 256 evaluations. Then, the transformation method requires that, for each  $\alpha$ -cut, all these models are evaluated obtaining for each of them the hypersurface of the output quantity, i.e. absorbed energy or total displacement, as a function of the process parameters, i.e. weight percentage of carbamide particles, mesh size of carbamide particles, and compaction speed. The fuzzy result for the given  $\alpha$ -cut is then obtained by computing the envelope of these hypersurfaces. In other words, the fuzzy model is able to describe, as the membership function decreases, an increasing number of experimental data and, thanks to the genetic algorithm, with the highest degree of belonging to the fuzzy set defined by the model itself. In particular, such a degree of belonging to the fuzzy set is ensured according to the fitness function:

$$f_v = w \cdot \frac{n}{N} + (1 - w) \cdot \frac{H_V}{H_C} \quad (3)$$

In the latter equation,  $f_v$  represents the fitness value,  $w$  represents a weighting term,  $n$  refers to the number of data not taken into account,  $H_V$  is the hypervolume covered by the combined fuzzy-genetic algorithm model and related to the uncertainty dispersion of the considered data. As reported in this equation, each term is opportunely normalized in order to have two comparable quantities. In particular, the first term is normalized by using the total number of the available data  $N$ , while the second term is normalized by using the hypercube including all the data,  $H_C$ .

Fig. 4. Genetic algorithm optimization: a)  $w = 0.1$ ; b)  $w = 0.3$ ; c)  $w = 0.5$ .

The use of such a fitness function is aimed at controlling the highest number of considered data in combination with the lowest hypervolume for the lowest level of membership. Fig. 4 shows the results of the genetic algorithm optimization for the absorbed energy. The experimental data are ordered for increasing value of absorbed energy obtained by the nominal regression model, represented as red asterisks, and the fuzzy model results, represented by the shaded area, where lighter zones refer to lower membership level. A similar result is obtained with respect to the compressive deformation, which is not reported for sake of brevity.

As shown in the latter figure, in all the cases it is possible to state that the nominal regression model (Equation 1) does not represent any experimental data (i.e. there are no experimental evaluation that can fall over the model surface). As the level of uncertainty is increased, measured by a decrease in the membership function, the model accommodates a larger number of samples with lower membership level. Moreover, increasing the weight  $w$ , both the number of data covered by the model and the width of the

fuzzy bands increase. However, Fig. 4a shows that a too low weight value involves very few data, while if it is too high (Fig. 4c) the dispersion of the fuzzy uncertainty bands is very large, even if the model is able to take into account almost all the experimental data. Among the different weight values investigated, the most suitable was 0.3. It is worth to note here that the uncertainty level related to the fuzzy model appears to be not constant with respect to the parameter combination used during the experimental tests. In fact, the extent of the input uncertainty in the model, due to the choice of a specific confidence interval, is not only related to the accuracy of the regression model adopted, but also to the variability of the process. This effect can be therefore considered the reason for a non-constant level of uncertainty.

In general, this kind of process maps can be used to select operational parameters in order to obtain a desired process output. They provide, as additional information, how much the uncertainty of the model and the process varies by changing operational parameters. This can be obtained by inverting the model and evaluating the best combination of the input parameters in order to satisfy the requirements of the highest energy absorption (set over 85% of the maximum) with the lowest compressive deformation (set below 40% of the highest level). This is useful for crashworthiness purposes. In fact, in crash situations, in order to ensure the safety of occupants inside a vehicle, the restraints structures should assure the highest absorption of the kinetic energy, minimizing crash loads transferred to the vehicle occupants, and on the same time these systems should control the deformation areas in order to maintain the adequate space in passenger cell and avoid intrusion of the surrounding structure.

The results can be represented in two-dimensional graphs by varying the input parameters one by one while fixing the others. In this way, different maps for each parameter combinations can be drawn. Fig. 5 shows the results obtained by applying the inverse fuzzy approach fixing the weight percentage of the carbamide to 40%, while varying the other two terms, i.e. the mesh size of the carbamide and the compaction speed. The membership level of the fuzzy model is represented as grey shaded area, while the experimental data and their occurrences as red dots (the dimension of each dot is proportional to the number of occurrences reported as green numbers respectively). The maps highlight that for  $C_{\%} = 40\%$ , in terms of energy absorption (Fig. 5a), it is possible to range along the whole axis of the compaction speed at the largest size of carbamide particles ( $C_{MS} = 20$ ) and along the whole axis of the mesh size at the highest compaction speed ( $S = 10$  mm/min). However, the best result is given by the combination of the highest value of  $S$  with the smallest size of  $C_{MS}$ , because it is characterized by the smallest uncertainty dispersion width and the darkest uncertain band. On the other hand, in terms of deformation (Fig. 5b), the requirement can be satisfied for any value, but in order to have the lowest uncertainty dispersion, the best combination is given by  $S = 1$  mm/min and  $C_{MS} = 12$ .

However, since the goal is to find the best solution that satisfy both requirements at the same time, the combination of the highest compaction speed and the smallest size of

carbamide particles can be considered the optimum, even if the fuzzy maps suggest that in this scenario the uncertainty is quite dispersed compared to the average nominal value (see Fig. 5c). It is worth to note that also from the experimental point of view this can be considered the most valuable solution, as highlighted by the occurrences reported as green number in Fig. 5c.

It is important to mention here that the fuzzy inverse maps obtained for the other parameters combinations are not reported because for increasing values of  $C_{\%}$  was not possible to satisfy the requirement of the highest energy absorption for values greater than 85%: the maximum absorption energy is about 55% of the highest value obtained in the experimental tests. This result can be attributed to the fact that increasing the percentage of the carbamide particles, there is an increase of the pores density of the foam and therefore a weaker structure is obtained.

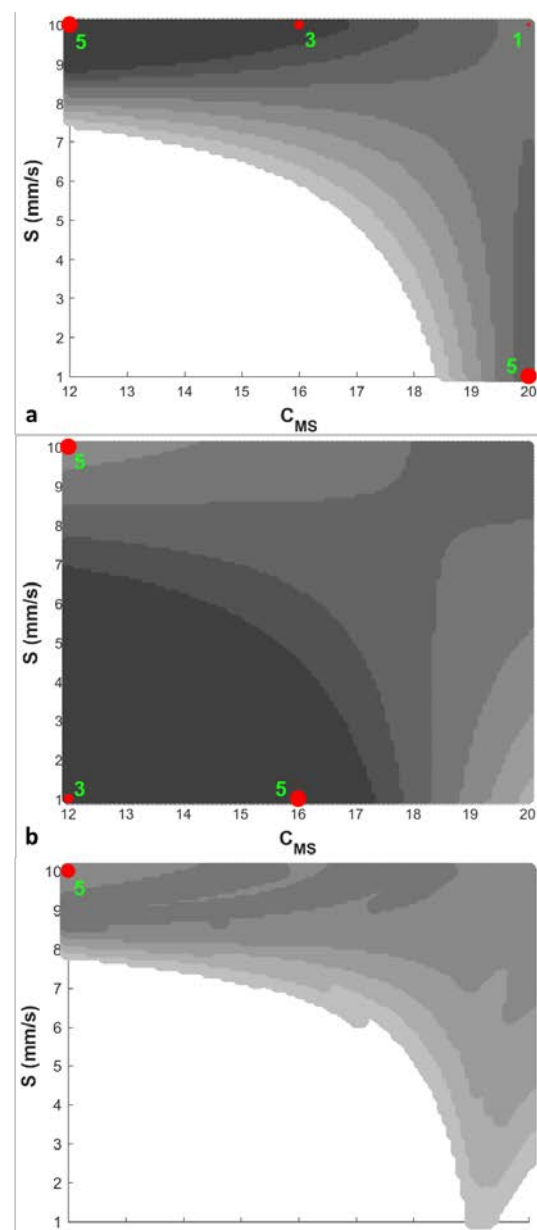


Fig. 5. Fuzzy inverse maps for  $C_{\%} = 40\%$  with: a)  $E > 85\%$ ; b)  $\Delta L < 40\%$ ; c) combination of  $E > 85\%$  and  $\Delta L < 40\%$ .

#### 4. Conclusions

In the present study a combined fuzzy-genetic algorithm methodology able to model the experimental data available from a metal foam manufacturing process was proposed. The aim was to select the manufacturing operational parameters in order to satisfy the requirements of the highest absorption of energy in combination with the lowest compressive deformation. In fact, for the purpose of energy absorption during crash of vehicles, it is necessary to maximize the energy absorbed during the impact while reducing the maximum deformation in order to maintain the adequate space in passenger cell. Moreover, the use of such a methodology gave as additional information how much the uncertainty of the model and the process varies by changing those operational parameters.

In particular, the input parameters were considered as triangular fuzzy numbers, and the Transformation Method was used to handle uncertainty propagation to the response variables. The genetic algorithm was used to optimize the support of each fuzzy parameter in order to find the best combination in terms of the maximum number of experimental data considered and the smallest hypervolume containing such data.

Inverting the model, by using the largest mesh size of carbamide particles and the highest compaction speed the best results in terms of energy absorption, deformation and uncertainty level can be achieved while using a 40% of carbamide. While, for greater values of carbamide particles percentage only a lower level of absorbed energy is achievable, i.e. the maximum absorption energy is about 55% of the highest value obtained in the experimental tests. This result can be attributed to the fact that increasing the percentage of the carbamide particles, there is an increase of the pores density of the foam and therefore a weaker structure is obtained.

In conclusion, as highlighted by the matching of the experimental results with the darkest areas of the fuzzy maps, which represents the most suitable combination of input parameters for a desired output, the fuzzy-genetic algorithm can be considered a valid and helpful tool in predicting, controlling and managing the output variables, proving to be practical for modelling complex and variable manufacturing processes.

#### References

- [1] Esen İ, Koç MA. Optimization of a passive vibration absorber for a barrel using the genetic algorithm. *Expert Syst Appl* 2015;42:894–905. doi:10.1016/j.eswa.2014.08.038.
- [2] Baiocco G, Ucciardello N. Neural network implementation for the prediction of secondary phase precipitation and mechanical feature in a duplex stainless steel. *Appl Phys A* 2019;125:20. doi:10.1007/s00339-018-2312-z.
- [3] Almonti D, Ucciardello N. Design and Thermal Comparison of Random Structures Realized by Indirect Additive Manufacturing. *Materials* (Basel) 2019;12:2261. doi:10.3390/ma12142261.
- [4] Wang Y, Zhai X, Wang W. Numerical studies of aluminum foam filled energy absorption connectors under quasi-static compression loading. *Thin-Walled Struct* 2017;116:225–33. doi:10.1016/j.tws.2017.03.032.
- [5] Ponticelli GS, Guarino S, Tagliaferri V, Giannini O. An optimized fuzzy-genetic algorithm for metal foam manufacturing process control. *Int J Adv Manuf Technol* 2019;101:603–14. doi:10.1007/s00170-018-2942-5.
- [6] Krastev V, Silvestri L, Falcucci G. A Modified Version of the RNG k-ε Turbulence Model for the Scale-Resolving Simulation of Internal Combustion Engines. *Energies* 2017;10:2116. doi:10.3390/en1022116.
- [7] Falcone D, Felice F De, Bona G Di, Duraccio V, Forcina A, Silvestri A. Validation and Application of a Reliability Allocation Technique (Advanced Integrated Factors Method) to an Industrial System. *Model. Identif. Control*, Calgary, AB, Canada: ACTAPRESS; 2014. doi:10.2316/P.2014.809-038.
- [8] Krastev VK, Silvestri L, Bella G. Effects of Turbulence Modeling and Grid Quality on the Zonal URANS/LES Simulation of Static and Reciprocating Engine-Like Geometries. *SAE Int J Engines* 2018;11:2018-01-0173. doi:10.4271/2018-01-0173.
- [9] Krastev VK, Silvestri L, Falcucci G, Bella G. A Zonal-LES Study of Steady and Reciprocating Engine-Like Flows Using a Modified Two-Equation DES Turbulence Model, 2017. doi:10.4271/2017-24-0030.
- [10] Rodger JA. Application of a Fuzzy Feasibility Bayesian Probabilistic Estimation of supply chain backorder aging, unfilled backorders, and customer wait time using stochastic simulation with Markov blankets. *Expert Syst Appl* 2014;41:7005–22. doi:10.1016/j.eswa.2014.05.012.
- [11] Rao RV. *Decision making in the manufacturing environment: using graph theory and fuzzy multiple attribute decision making methods*. Springer; 2007.
- [12] Almonti D, Simoncini M, Tagliaferri V, Ucciardello N. Electrodeposition of graphene nanoplatelets on CPU cooler—experimental and numerical investigation. *Mater Manuf Process* 2018;33:220–6. doi:10.1080/10426914.2017.1303165.
- [13] Almonti D, Ucciardello N. Improvement of thermal properties of micro head engine electroplated by graphene: experimental and thermal simulation. *Mater Manuf Process* 2019;1-8. doi:10.1080/10426914.2019.1594263.
- [14] Lamata MT, Pelta D, Verdegay JL. Optimisation problems as decision problems: The case of fuzzy optimisation problems. *Inf Sci (Ny)* 2018;460-461:377–88. doi:10.1016/j.ins.2017.07.035.
- [15] Zadeh LA. *Fuzzy Sets*. *Inf Control* 1965;8:338–53.
- [16] Ashby MF, Evans AG, Fleck NA, Gibson LJ, Hutchinson JW, Wadley HNG. *Metal Foams: A Design Guide*. 2000.
- [17] Guarino S, Barbieri M, Pasqualino P, Bella G. Fabrication and Characterization of an Innovative Heat Exchanger with Open Cell Aluminum Foams. *Energy Procedia* 2017;118:227–32. doi:10.1016/j.egypro.2017.07.015.
- [18] Barbieri M, Di Ilio G, Patanè F, Bella G. Experimental investigation on buoyancy-induced convection in aluminum metal foams. *Int J Refrig* 2017;76:385–93. doi:10.1016/j.ijrefrig.2016.12.019.
- [19] Chiappini D. Numerical simulation of natural convection in open-cells metal foams. *Int J Heat Mass Transf* 2018;117:527–37. doi:10.1016/j.ijheatmasstransfer.2017.10.022.
- [20] Guarino S, Ilio G Di, Venettacci S. Influence of Thermal Contact Resistance of Aluminum Foams in Forced Convection: Experimental Analysis. *Materials* (Basel) 2017;10:907. doi:10.3390/ma10080907.
- [21] Kremer K. *Metal Foams for Improved Crash Energy Absorption in Passenger Equipment*. 2004.
- [22] Barletta M, Gisario A, Guarino S, Rubino G. Production of Open Cell Aluminum Foams by Using the Dissolution and Sintering Process (DSP). *J Manuf Sci Eng* 2009;131:041009. doi:10.1115/1.3159044.
- [23] Hanss M. The transformation method for the simulation and analysis of systems with uncertain parameters. *Fuzzy Sets Syst* 2002;130:277–89.
- [24] Goodall R, Marmottant A, Salvo L, Mortensen A. Spherical pore replicated microcellular aluminium: Processing and influence on properties. *Mater Sci Eng A* 2007;465:124–35. doi:10.1016/j.msea.2007.02.002.
- [25] Montgomery DC. *Introduction to Statistical Quality Control*. Sixth Edit. Wiley; 2009.